Electronic transport in molecular-beam-epitaxy-grown $Al_xGa_{1-x}As$

M. Zachau and F. Koch
Physik-Department, Technische Universität München, D-8046 Garching bei München, Federal Republic of Germany

G. Weimann and W. Schlapp
Forschungsinstitut der Deutschen Bundespost, D-6100 Darmstadt, Federal Republic of Germany

(Received 17 December 1985)

We have studied magnetotransport and cyclotron resonance of electrons in interfacial subbands of a series of remote-doped $Al_{0.35}Ga_{0.65}As$-$Al_xGa_{1-x}As$ heterostructures with x up to 0.26. The experiments allow an accurate determination of $m_c^*(x)$ and define an upper limit of the strength of the alloy disorder scattering.

I. INTRODUCTION

Much effort has gone into the study of electron transport in GaAs surface subbands facing an n-type doped $Al_xGa_{1-x}As$ barrier. Scattering mechanisms and the transport effective mass of such GaAs electrons have been thoroughly explored in experiment and theory.

There is a new generation of "band-structure-engineered" devices being considered for future applications that involve carrier transport in $Al_xGa_{1-x}As$ with varying x. This provided the incentive and motivation for the present experiments which explore the electron mass and transport mobility in MBE- (molecular-beam epitaxy) grown $Al_xGa_{1-x}As$.

The literature gives the band-edge mass m_0^* and its variation with x as $m_0^*/m_0=0.066+0.088x$ (Ref. 1) and $m_0^*/m_0=0.067+0.083x$ (Ref. 2). Such dependences have been derived through a fit to magnetotransport data. The only direct measurements are unpublished cyclotron-resonance experiments,[3] which used n-type doped LPE- (liquid-phase epitaxy) grown layers. By contrast, we have chosen to examine the surface subbands of a remote-doped heterostructure with the $Al_xGa_{1-x}As$ interfacing to another layer with higher Al content. The high mobility of the channel electrons in the heterostructure allows a better determination of the cyclotron mass, one that is not affected by impurity binding. Using the density N_s measured from the oscillatory magnetoconductivity of the two-dimensional electron gas (2DEG) the cyclotron mass can be referred back to an m_0^* for $Al_xGa_{1-x}As$. Because of the reduced ionized donor scattering in the heterostructure we can define a meaningful upper limit of the strength of the alloy scattering.

II. SAMPLES AND THEIR SUBBAND STRUCTURE

The heterostructures are grown on semi-insulating GaAs substrates. The layer sequence is 1 μm of GaAs as a buffer, 1 μm of undoped $Al_xGa_{1-x}As$, and then the barrier-interface layer with the higher $x\simeq 0.35$. The first 60 Å of the latter is an undoped spacer. There follows 400 Å of n-type doped barrier material. The structure is protected by a thin capping layer of GaAs.

Altogether, samples with five different interface compositions are employed in the experiments. The parameters are given in the upper part of Fig. 1. The barrier for all but the last of the interfaces is a constant $x\simeq 0.35$ material. Only because all attempts at making an $x=0.26$ sample with carrier density and mobility comparable to the other samples failed, we choose the higher $x=0.50$ barrier for this case. We thus obtain data for four different x values.

Because of the nonparabolicity of the $Al_{1-x}Ga_xAs$ conduction band, the measured subband cyclotron mass m_c^* lies above $m_0^*(x)$. To relate m_c^* to m_0^*, we require a calculation of the surface bands. Measurements of m_c^* are made under illumination with band-gap radiation, providing high N_s and guaranteeing a vanishingly small de-

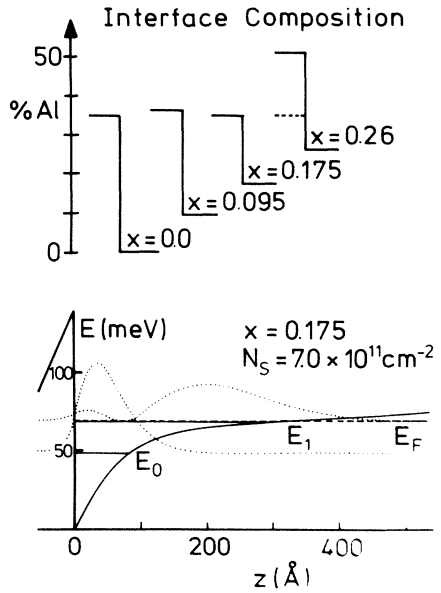

FIG. 1. Interface composition for the five different types of heterostructures. The resulting subband energy and wave function for the occupation N_s observed for the $x=0.175$ sample are shown in the lower half ($N_{depl}=10^{10}$ cm^{-2}).

pletion field in the active $Al_xGa_{1-x}As$ layer. The calculation is done for quasiaccumulation with $N_{depl}=1\times10^{10}$ cm^{-2} and follows the approach of Ando.[4] Image-potential effects are ignored and many-body corrections in the subband energy are calculated according to Ref. 5. The mass enhancement caused by nonparabolicity is taken in the form[4]

$$\frac{\Delta m^*}{m_0^*}\simeq\left[1+\frac{4(\langle K\rangle_0+E)}{E_g}\right]^{1/2}-1\ ,$$

where $E_g(x)$ is the band gap, $\langle K\rangle_0$ the kinetic energy of the ground-state subband, and E the energy of parallel motion in that band.

The subbands are calculated for the N_s measured in the ground state. The energy E_0 (also E_1 when the $n=1$ subband is occupied), wave function, self-consistent potential, and Fermi energy E_F are determined using the band offset 0.65×1.24 eV$\times\Delta x$ at the interface. The energy barrier controls the penetration of the wave function into the high-x material. It influences $\langle K\rangle_0$ and, via the nonparabolicity expression, also Δm^*. Quantitatively, this contribution to Δm^* is small. Penetration also implies that the mass is increased because the carrier is, in part, in the high-x material. Again, the correction is so small that the uncertainty in the barrier offset does not effect m_c^* beyond the experimental accuracy.

An example of the calculated surface bands for the $x=0.175$ sample is given in the lower half of Fig. 1. According to the calculation 2.4% of the total surface charge is taken up in the $n=1$ band.

III. MAGNETOTRANSPORT EXPERIMENTS

We measure the conductivity $\sigma_{xx}(B)$ in the Corbino-disk geometry by the capacitive-coupling technique.[6] The density N_s is evaluated from the oscillation period of data such as that in Fig. 2. For the $x=0.175$ sample only the ground-state occupancy of 7.0×10^{11} cm^{-2} can be determined reliably.

The mobility of the interface carrier is obtained by fitting σ_{xx} to the relation $\sigma_0/(1+\mu^2B^2)$. The value agrees within the experimental accuracy of 2–3 % with that derived from the measured σ_0 divided by N_se. The calculated 2.4% occupancy of the $n=1$ state is not detected. Moreover, this contribution to σ_{xx} depends sensitively on the leakage of the wave function into the barrier. The $\sigma_\square$ plotted in Fig. 2 has a small background contribution from a bypass in the doped barrier material. It is marked by the dashed line in Fig. 2, fixed such that $\sigma_{xx}(B)$ has the expected classical functional form.

The channel density N_s can be increased in steps from some low value by the cumulative effect of light pulses. We generally find an increasing μ with N_s in each of the samples studied. Figure 3 shows data for the $x=0.095$ and 0.175 samples.

A rising μ versus N_s is usually associated with Coulomb scattering. In Refs. 7 and 8 the N_s dependence of this contribution has been calculated under certain restrictive conditions. Reference 9 shows that, in practice, for heterojunction transport in GaAs for some samples, a slower increase at high N_s can be observed. Ando's calculation of Coulomb-scattering limited mobility μ_C for a constant density of dopant atoms in the barrier material serves as a guide for what may be expected for the present samples. With a 60-Å spacer and the known doping level of the two samples we calculate the dashed lines for $\mu_C(N_s)$ in Fig. 3. Both samples have a mobility which lies below this Coulomb-scattering result.

Alloy disorder scattering is described in the theory of Ref. 10 in terms of a contact interaction, where the density of the electron at the site of the statistically fluctuating potential is the relevant factor. This density increases with N_s.

If we now assume that alloy scattering alone accounts for the difference between the calculated Coulomb scattering μ_C and the measured μ, we obtains from Mathiessen's rule the straight line marked μ_A for the $X=0.175$ sam-

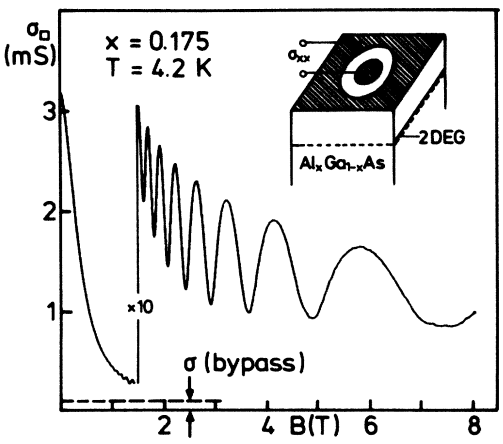

FIG. 2. Magnetoconductivity $\sigma_\square$ for the $x=0.175$ sample as measured with the capacitive-coupling, Corbino-disk geometry (inset). The dashed line gives the field-independent contribution to $\sigma_\square$ of a bypass in the barrier.

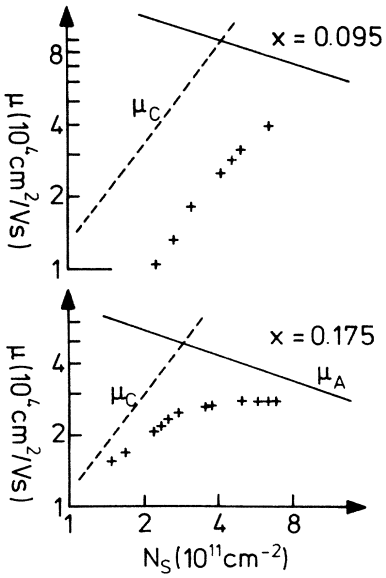

FIG. 3. Mobility vs carrier density for two samples. The experimental values are given by pluses.

ple. For this case it has the functional form required of alloy scatteirng. Its magnitude gives the strength of the scattering potential as $\langle V_A \rangle = 0.88$ eV. We realize that this particular sample may represent a lucky coincidence. Its luminescence characteristic showed it to be particularly free of background contaminants. Since interface-roughness scattering also decreases μ with rising N_s, $\langle V_A \rangle$ is likely to be an overestimate, an upper limit to the strength of the disorder scattering.

The comparison with the data on the $x = 0.095$ sample in the upper part of Fig. 3 shows that, in general, we cannot expect to analyze the mobility solely in terms of Ando's μ_C (for constant doping) and a μ_A. When we scale down the latter according to $x(1-x)(m_c^*)^{-7/3}$, the solid line in the upper part of the figure results. The calculated μ_C is the dashed line. The observed mobility lies substantially lower than expected from the sum of the scattering rates. The luminescence signal in this case showed some unintentional background contamination.

IV. CYCLOTRON RESONANCE

The mass m_c^* of the subband electrons is obtained from cyclotron resonance in the Faraday geometry. Experimental curves of the transmisison of linearly polarized 10.45 meV radiation versus B are shown in Fig. 4. The data were fitted to standard expressions[11] using the measured density N_s, in order to extract m_c^* and the relaxation parameter $\omega\tau$. The $\omega\tau$ values for the resonance experiments are consistently lower than those calculated from the mobility data. The difference amounts to about

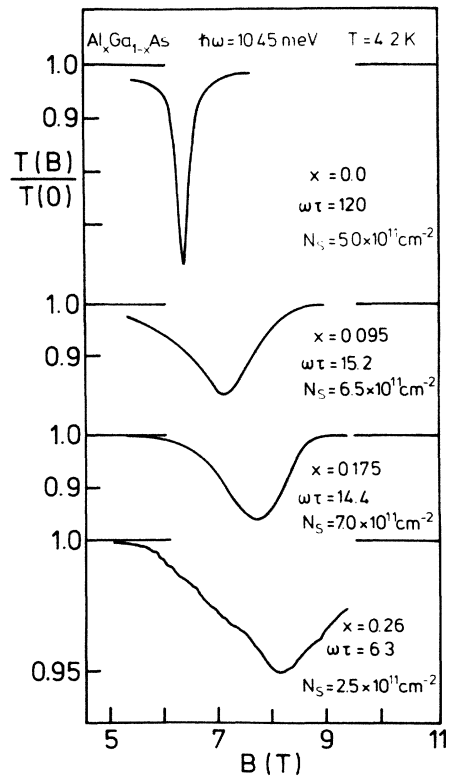

FIG. 4. Cyclotron resonance observed as a change of the transmitted intensity for the various alloys.

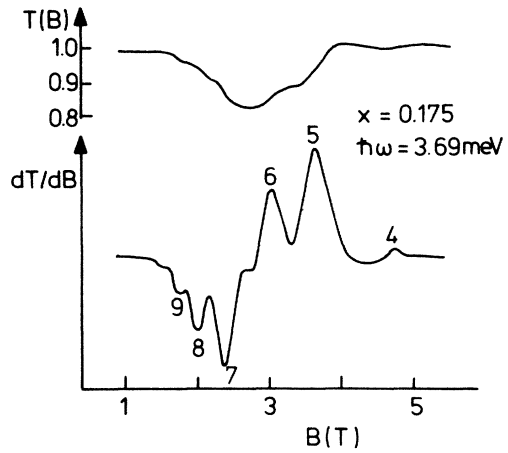

FIG. 5. Cyclotron resonance and its derivative for the $x = 0.175$ sample and $\hbar\omega = 3.69$ meV. The numbers give the Landau-level index.

30% for the present data and is generally attributed to a modification of the scattering dynamics in a strong magnetic field. The signal amplitude is a sensitive function of N_s and the good agreement achieved with the simple transmission formula, as well as the absence of typical line-shape distortion, show that parallel-plate interference effects can be neglected.

The nonparabolicity correction involves the energy E of parallel motion. In the case of quantum transitions between Landau levels l and $l+1$, the observed mass represents the value at an energy just midway between the levels. The lines for the $x = 0.095$ and 0.175 alloy samples are sufficiently wide to include during the B-sweep quantum transitions symmetrically from $\hbar\omega$ below to $\hbar\omega$ above the energy E_F. In this case the measured m_c^* represents the mass for $E = E_F$. For the $x = 0.26$ sample and the smaller occupancy of $N_s = 2.5\times10^{11}$ cm^{-2}, we have at the resonance field of 8.15 T a quantum limit situ-

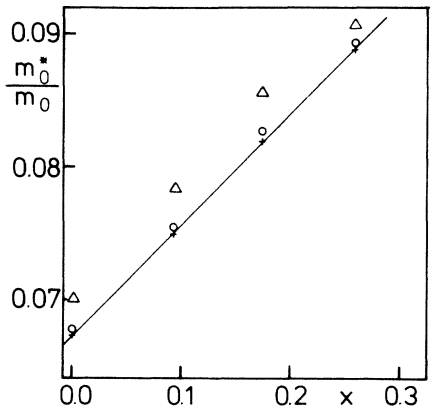

FIG. 6. Experimental values of m_c^* vs x measured at $\hbar\omega = 10.45$ meV (cf. Fig. 4) are given by the points marked Δ. After a nonparabolicity correction for subband and parallel-motion energies, one obtains the masses given by ○. A further correction for the penetration of electrons into the barrier gives the masses marked by +. The line gives the band-edge mass $m_0^*(x)$.

ation. Ignoring spin, the measured m_c^* is a mass value for $E=\hbar\omega=10.45$ meV.

The fact that several quantum transitions contribute to the resonance is nicely demonstrated with the observation of the so-called Ando oscillations in the resonance line. The effect was first seen in Si experiments[11] for parameter values N_s and $\omega_c\tau$ that resemble those for the data in Fig. 5 below. At the low energy of $\hbar\omega=3.69$ meV, the $x=0.175$ sample resonance includes transitions between the many Landau levels marked on the figure.

Figure 6 finally summarizes the m_c^* data. Triangles mark the measured value with an estimated uncertainty comparable to the symbol size. The nonparabolicity correction for the subband and parallel motion energies leads to values marked with a circle. The barrier penetration effect (calculated with the 65—35% rule of band offset) gives a further correction to the value marked by pluses. This represents finally the band-edge mass $m_0^*(x)$. The straight line represents

$$m_0^*=(0.067+0.0838x)m_0 \ .$$

The slope of m_0^* versus x is significantly greater than that found for the resonance experiments in Ref. 3. The present results, which to our knowledge are the first cyclotron-resonance measurements of $m_c^*(x)$ in heterostructures, agree very well with the value in Ref. 2.

ACKNOWLEDGMENTS

This work has been supported by the Deutsche Forschungsgemeinschaft (Sonderforschungsbereich 128).

[1]H. J. Lee, L. Y. Juravel, J. C. Woolley, and A. J. Spring Thorpe, Phys. Rev. B **21**, 659 (1980).
[2]N. Lifshitz, A. Jayaraman, R. A. Logan, and H. C. Card, Phys. Rev. B **21**, 670 (1980).
[3]W. Ossau, Ph.D. thesis, University of Würzburg, 1982.
[4]T. Ando, J. Phys. Soc. Jpn. **51**, 3893 (1982).
[5]F. Stern and S. Das Sarma, Phys. Rev. B **30**, 840 (1984).
[6]V. Dolgopolov, C. Mazuré, A. Zrenner, and F. Koch, J. Appl. Phys. **55**, 4280 (1984).
[7]T. Ando, J. Phys. Soc. Jpn. **51**, 3900 (1982).
[8]W. Walukiewicz, H. E. Ruda, J. Lagowski, and H. C. Gatos, Phys. Rev. B **30**, 4571 (1984).
[9]G. Weimann and W. Schlapp, Appl. Phys. Lett. **46**, 411 (1985).
[10]G. Bastard, Appl. Phys. Lett. **43**, 591 (1984).
[11]G. Abstreiter, J. P. Kotthaus, J. F. Koch, and G. Dorda, Phys. Rev. B **14**, 2480 (1976).